Journal of Alloys and Compounds 323–324 (2001) 842–846
www.elsevier.com/locate/jallcom

Laser-induced time-resolved luminescence as a means for discrimination of oxidation states of Eu in minerals

M. Gaft[a,*], R. Reisfeld[b], G. Panczer[c], O. Ioffe[d], I. Sigal[d]

[a]Department of Natural Science, The Open University of Israel, 16 Klausner St., Tel-Aviv, Israel
[b]Department of Inorganic and Analytical Chemistry, Hebrew University, 91940, Jerusalem, Israel
[c]Physical Chemistry of Luminescence Materials Laboratory, Lyon 1 University and CNRS, 43 Bd. Du 11 November 1918, 69622 Villeurbanne, France
[d]Geological Survey of Israel, Jerusalem, Israel

Abstract

Simultaneous detection of divalent and trivalent europium is investigated by time-resolved laser-induced luminescence in a number of minerals. The selectivity of detection is possible by using different time delays after excitation, different gate widths and different excitation wavenumbers. This technique allows detection of Eu luminescence in minerals in which it is hidden by other luminescence centers in the steady-state luminescence spectra. In such a manner we detected Eu^{2+} and two different Eu^{3+} luminescence centers in apatite and fluorite, Eu^{2+} and Eu^{3+} luminescence in datolite and danburite, and Eu^{3+} luminescence in zircon and calcite. © 2001 Elsevier Science B.V. All rights reserved.

Keywords: Luminescence; Time-resolved; Europium; Apatite; Minerals

---

1. Introduction

Trivalent europium is an excellent ionic probe for materials and its luminescence properties are extensively studied. Eu is one of the mostly informative elements in mineralogy, especially when the ratio Eu^{2+}/Eu^{3+} may be assessed. Both oxidation states are luminescent, but the lines of Eu^{3+} in minerals are usually very weak and concealed by another centers. Using steady-state luminescence spectroscopy its luminescence has been confidently detected only in scheelite [1,2].

The energy levels of Eu^{3+} arise from the $4f^n$ configuration. In a configuration coordinate diagram these levels appear as parallel parabolas ($\Delta R=0$), because the 4f electrons are well shielded by the $5s^2 5p^6$ outer shells and the crystal field influence is weak. The emissions arising from f–f transitions yield sharp lines in the spectra. Because the transitions occur between states of the same parity, the lifetime of the excited state is long. The emission in Eu^{3+} corresponds to transitions from excited $^5D_0$ level to the ^7F_J ($J=0, 1, 2, 3, 4, 5, 6$) levels of the $4f^6$ configuration. Because the $^5D_0$ level is not split by the crystal field (because $J=0$), the splitting of the emission transition lines yields the crystal field splitting of the ^7F_J levels. If Eu^{3+} occupies a crystal lattice site with inversion symmetry, optical transitions between levels of the $4f^n$ configuration are strictly forbidden as electric-dipole transitions (parity selection rule). They can only occur as the much weaker magnetic-dipole transitions which obey the selection rule $\Delta J=0, \pm 1$ (but $J=0$ is forbidden) or as vibronic electric-dipole transitions. If there is no inversion symmetry at the site of Eu^{3+}, the uneven crystal field components can mix opposite-parity states into $4f^n$ configurational levels. The electric-dipole transitions are now no longer strictly forbidden and appear as weak lines in the spectra, the so-called forced electric-dipole transitions. Some-transitions, viz. with $\Delta J=\pm 2, \pm 4$, are hypersensitive to this effect. Even for small deviations from inversion symmetry, they appear dominantly in the spectrum [3,4].

In the group of divalent RE luminescence centers, Eu^{2+} is the most well known. It shows a 5d–4f emission which varies in minerals from UV to blue. Its decay time is about 600–800 ns. This is due to the fact that the emitting level contains spin octets and sextets, whereas the ground state level (^8S from $4f^7$) is an octet, so that the optical transition rate is slower because of spin selection rule. The host lattice dependence of the emission color of the Eu^{2+} is

---

*Corresponding author. Tel.: +972-3-6460-549; fax: +972-3-6460-582.

E-mail address: michael@shaked.openu.ac.il (M. Gaft).

PII: S0925-8388(01)01157-4

Table 1
Luminescent RE concentrations (ppm) in minerals with detected Eu emission

	Ce	Pr	Nd	Sm	**Eu**	Gd	Tb	Dy	Ho	Er	Tm
Apatite Green	519	63	237	50	**12**	40	7	41	9	24	4
Apatite Blue	4052	424	1470	199	**28**	133	14	59	11	25	3
Apatite White	1020	327	1119	160	**41**	90	15	64	8	23	2
Apatite Red	1367	156	583	134	**37**	208	23	72	13	46	4
Scheelite USA	100	11	42	10.0	**35**	11	2	13	2.0	8.0	1
Zircon Kola	68	10	63	48.0	**25**	143	40	352	96	300	56
Calcite Russia	41	5.0	18	4.0	**22**	6.0	1	6	1	2	0.5
Fluorite France	280	57	370	200	**28**	280	55	350	70	220	35
Fluorite Russia	33	5	26	12	**6.5**	22	4.0	27	5.5	14	1.7
Anhydrite	2.3	0.3	1.7	0.6	**0.3**	0.8	0.2	0.7	0.2	0.4	0.1
Danburite	3	0.3	1.0	0.2	**1**	0.1	–	0.1	–	–	–
Datolite	22	3	11	2	**0.5**	1.7	0.2	1	0.2	0.7	0.1
Xenotime	745	65	380	195	**33**	385	75	545	135	415	55

mainly connected with covalency (the nephelauxetic effect) which will reduce the energy difference between the 4f and 5d configurations, crystal field splitting of the 5d configuration and the Stokes shift [4].

The purpose of this work is to examine different minerals by laser-induced time-resolved luminescence, which allows differentiation between luminescence centers with emission spectra in the same spectral range but with different decay times. The method involves recording the intensity in a specific time gate at a given delay after the excitation pulse, where both the delay and gate width have to be carefully chosen. Time-resolved spectroscopy allows detection of the previously unseen emission lines of europium, which were present but hidden under other luminescence and not differentiated in steady-state spectra.

2. Experimental

The luminescence spectra were investigated under third and fourth harmonics of YAG (266 and 355 nm) and nitrogen (337 nm) laser excitations. The spectra were analyzed by InstaSpec IV CCD detection system, which enables computer controlled acquisition of time-resolving spectra with delay times and strobe pulse duration from 20 ns to 9 ms.

This paper is based on luminescence of different minerals, which exhibit characteristic lines and bands of Eu^{3+} and Eu^{2+}. RE concentrations in minerals under study were determined by us using inductively coupled plasma analysis (Table 1).

3. Results

3.1. Apatite $Ca_5(PO_4)_3$(F, Cl, OH)

Divalent europium is detected in apatite as a shoulder of Ce^{3+} luminescence when studied by steady-state spectroscopy [1,2]. The reason is that Eu^{2+} and Ce^{3+} luminesce in the same spectral range, but the Eu concentration in all investigated samples is very low compared to that of Ce (Table 1). Besides that, since the 5d–4f transition in Ce^{3+} is parity allowed and spin selection is not appropriate, the emission transition is fully allowed one and luminescence intensity is very strong. Thus Ce^{3} makes Eu^{2+} luminescence detection hardly possible. However, because Eu^{2+} has a much longer decay time, time-resolved spectroscopy enables the isolation of the Eu^{2+} luminescence in pure form. After a delay of 100 ns and with a gate width of 500 ns, the short-lived luminescence of Ce^{3+} is already quenched and the long-lived luminescence of other trivalent RE and Mn^{2+} is not detected yet. At such conditions the blue, relatively narrow band peaking at 450 nm appears with intermediate decay time of ~400 ns (Fig. 1a). Such an emission band is known as in natural and in synthetic artificially activated apatite and is connected with Eu^{2+} [1]. On excitation with UV, two types of lowest excited states are possible, namely ^6P_J (f–f) or $4f^6 5d$ (f–d), depending on the host matrix. The nature of Eu^{2+} emission, namely either an intra-configurational (f–f) line or inter-configurational (f–d) band emission in a given host, is mainly decided by the effect of the ligand field on the Eu^{2+} energy levels. In the apatite case, the anions constituted by the PO_4^{3-} network produce a strong nephelauxetic effect and hence the $4f^6 5d$ level is the lowest excited state, leading to band emission. It was found that in calcium fluor-apatite there is only one emission band. The emission maximum dependence on the halogen type confirms that this band can be assigned to the Ca(II) sites [5].

Luminescence of Eu^{3+} was not detected in steady-state spectra. By laser-induced time-resolved spectroscopy, emission lines of Eu^{3+} at 617, 651 and 695 nm have been detected in apatite in the high symmetry Ca(I) position [6]. They are especially prominent under 266 nm excitation (Fig. 1b). Besides that, under 337 and 355 nm excitations new lines at 576 and 632 nm appear (Fig. 1c). They are known in synthetic artificially activated apatite and connected with Eu^{3+} in the low symmetry Ca(II) site [6], but

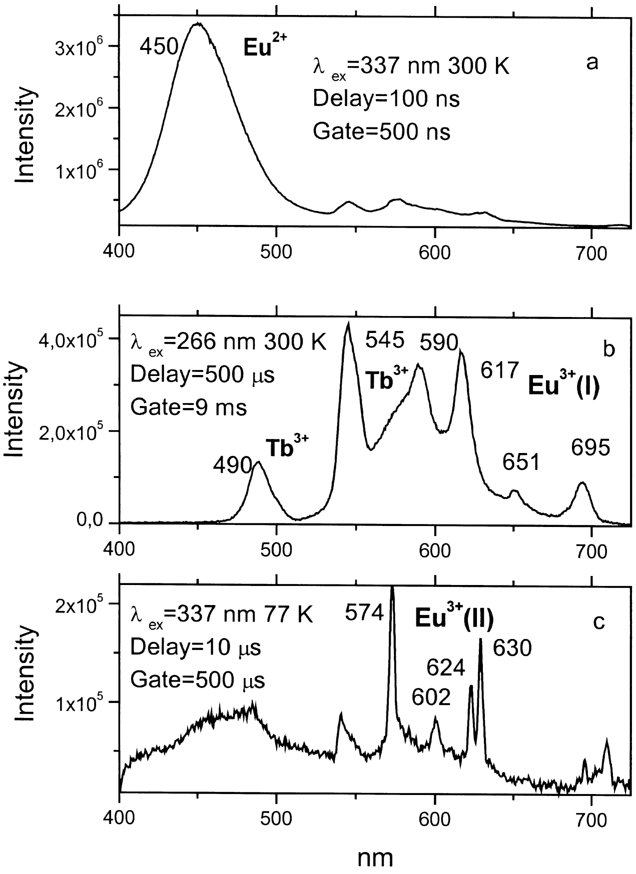

Fig. 1. Laser-induced time-resolved luminescence spectra under different excitations of apatite with red color (Norway). Eu^{3+}(I) denotes the substitution in a high symmetry Ca(I) site, while Eu^{3+}(II) denotes the substitution in a low symmetry Ca(II) site.

have never been detected in natural apatite. Because of the lower symmetry of Eu^{3+} in the Ca(II) site its luminescence has a relatively short decay time and is more prominent in the spectrum with a narrower gate width. This center is especially strong at liquid nitrogen temperature where the prominent $^5D_0$–$^7F_0$ line of Eu^{3+} at 574 nm is seen, unhidden by Dy^{3+} luminescence the relative intensity of which is substantially lower at 77 K.

3.2. Fluorite CaF_2

The luminescence center of divalent europium in fluorite is well known [2]. However, the luminescence of Eu^3 has not been detected in natural samples using steady-state spectroscopy, because it is obscured by the strong emission band of Eu^{2+} (Fig. 2a). Because the decay time of Eu^{2+} is in the range of 600–800 ns, it is already quenched after a delay of 10 µs and only the long-lived luminescence of RE^{3+} is detected. Two groups of lines appear, which may be ascribed to Eu^{3+}: the first at 595, 622, 645 and 702 nm and the second at 574, 618 and 633 nm with the main line at 574 nm (Fig. 2b,c). Two types of RE luminescence centers are well known in synthetic artificially activated fluorite [7]. Eu^{3+} may be located in the CaF_2 lattice in several non-equivalent positions with cubical, tetragonal, trigonal and rhombic symmetries. Decay times of the first group of luminescence lines are extremely long, possibly indicating high symmetry cubic symmetry. Another group of Eu^{3+} lines with shorter decay time is connected with a Eu^{3+} site of lower symmetry in fluorite lattice. The Eu^{3+} line at 574 nm belongs to $^5D_0$–$^7F_0$ transition which exists only in cases where the site symmetry allows an electric dipole process: C_s, C_n, C_{nv} [3,4].

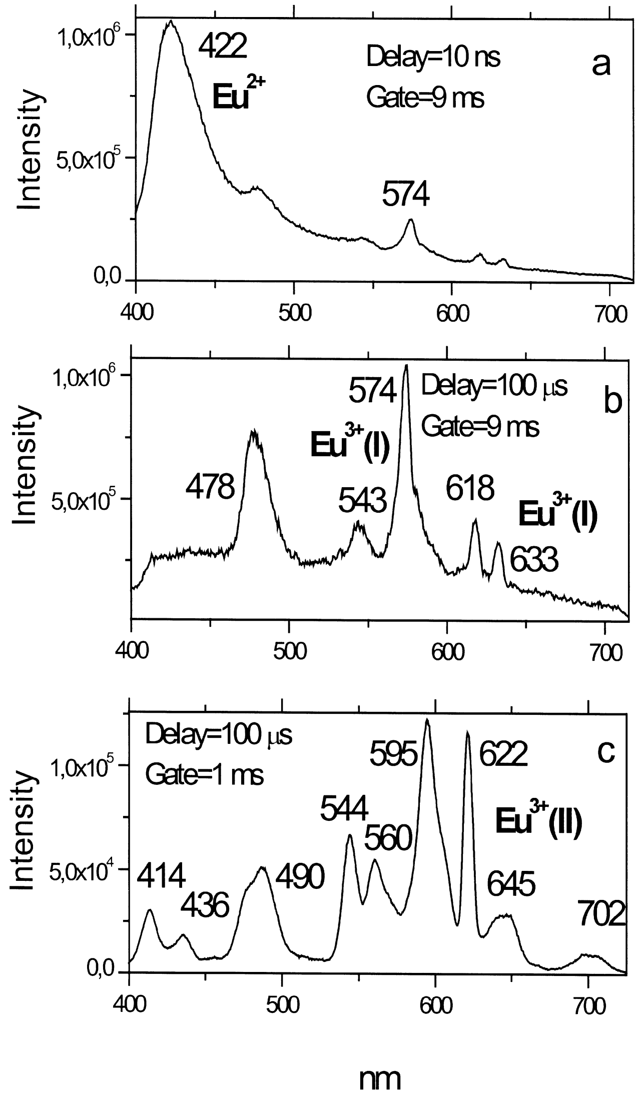

Fig. 2. Laser-induced time-resolved luminescence spectra under $\lambda_{ex}=266$ nm of fluorite samples from France (a) and Russia (b,c). Eu^{3+}(I) denotes the substitution in a high symmetry position, while Eu^{3+}(II) denotes the substitution in a low symmetry position.

3.3. Zircon $ZrSiO_4$ and Xenotime YPO_4

Luminescence spectra of natural zircon are characterised by broad-band yellow emission [2]. The RE luminescence is not detected under steady-state conditions. A relatively short delay time of 100 μs allows to weaken zircon's broad bands with their shorter decay of 10–30 μs and to detect the lines of Dy^{3+} at 480 and 575 nm. A longer delay times of 1–2 ms enables the yellow bands to extinguish and the detection of the long-lived Sm^{3+} and Eu^{3+} luminescence (Fig. 3a). The connection of the detected lines with Eu^{3+} was confirmed by the study of synthetic $ZrSiO_4$-Eu, where three main sites have been detected [8]. The lines detected in natural zircon belong to the Eu^{3+}(II) site with a long decay time.

Synthetic YPO_4-Eu^{3+}, which has the zircon-type structure, is a well-known commercial phosphor. In natural xenotime the strong uranyl luminescence covers Eu^{3+} lines in the steady-state spectra. The shorter decay time of uranyl, compared to that of Eu^{3+}, enables one to detect the Eu^{3+} luminescence after a delay time of 1 ms (Fig. 3b). Similar behavior is demonstrated by thorite $ThSiO_4$, orangite (orange variety of thorite) and monazite (Ce, La, Y, Th).

3.4. Barite $BaSO_4$ and anhydrite $CaSO_4$

Luminescence of Eu^{2+} is well known in these minerals [2]. It is interesting to note that the Eu^{2+} band often appears in barite after heating in air at 600–700°C. It is the result of some kind of transformation which takes place in the barite lattice under these conditions. Several possibilities exist. In barite the Eu^{2+} luminescence might be quenched by the components with high-energy phonons (e.g., water and/or organic matter). If they are removed by heating, then the Eu^{2+} luminescence becomes visible.

The following scenario is also a possibility. Eu initially enters the barite lattice in the form of Eu^{+}, which oxidizes to Eu^{2+} at 700°C. The relatively small difference between the Ba^{2+} and the Eu^{+} ionic radii (1.5 and 1.7 Å, correspondingly) makes this substitution possible under the conditions of charge compensation.

Luminescence of Eu^{3+} is found in anhydrite under 266 nm excitation. Luminescence lines at 593 and 619 nm evidently belong to Eu^{3+} (Fig. 4b).

3.5. Datolite $CaBSiO_4(OH)$ and Danburite $CaB_2(SiO_4)$

Luminescence of Eu^{2+} was found by steady-state luminescence spectroscopy in these minerals [9]. Time-resolved luminescence spectroscopy allowed detection of

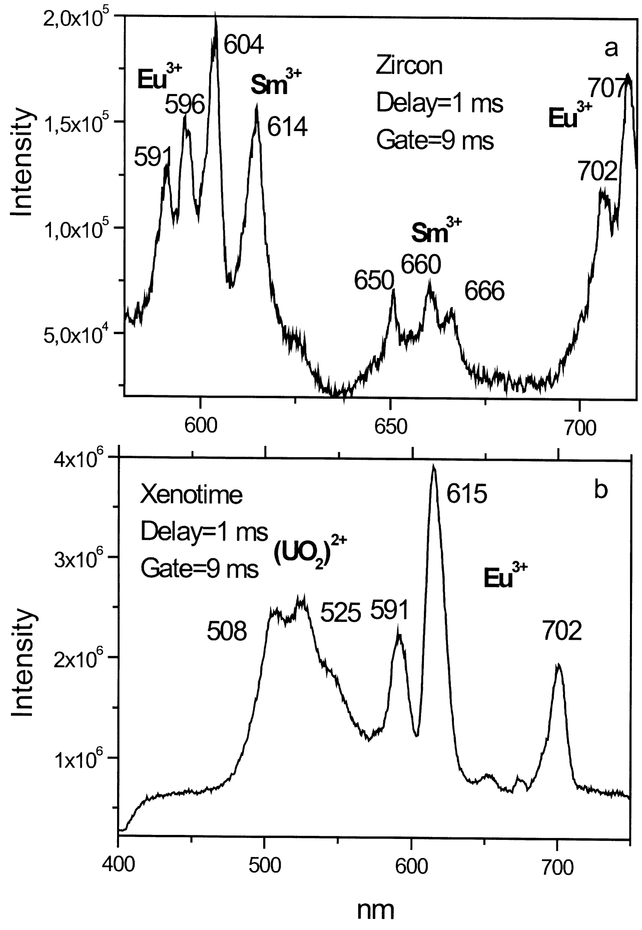

Fig. 3. Laser-induced time-resolved luminescence spectra under λ_{ex}=266 nm of zircon (Kola, Russia) (a) and xenotime (Norway) (b).

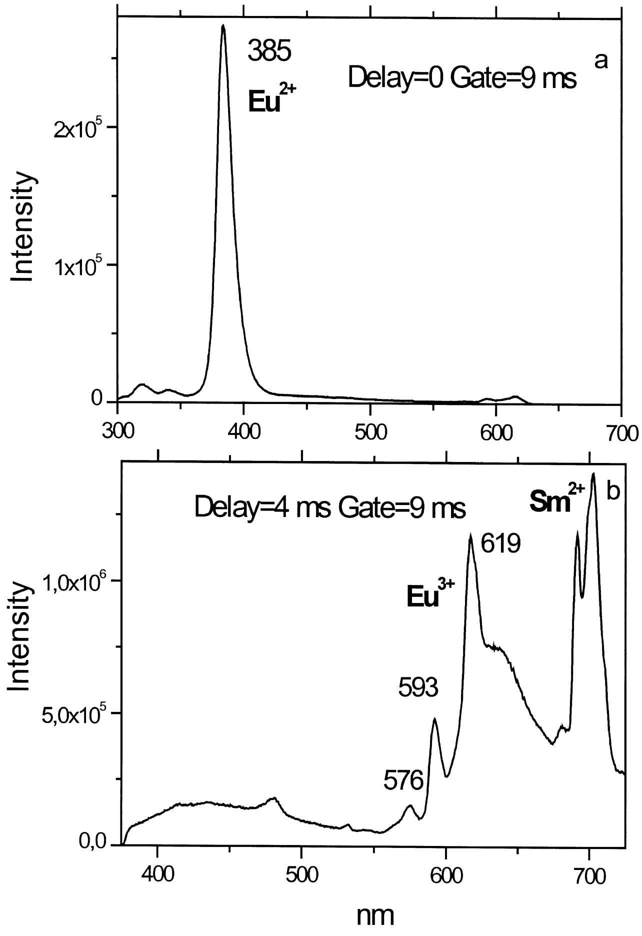

Fig. 4. Laser-induced time-resolved luminescence spectra under λ_{ex}=266 nm of anhydrite.

luminescence lines at 580, 598, 611, 655 and 691 nm in danburite (Fig. 5b) and at 578, 600, 610, 619 and 700 nm in datolite, all of which evidently belong to Eu^{3+}.

3.6. Calcite $CaCO_3$

Laser-induced time-resolved luminescence of calcite under 266 nm excitation with little delay is connected with a strong radiation-induced violet band. After a delay of 100 μs, luminescence lines at 590, 618 and 697 nm appear which evidently belong to Eu^{3+} (Fig. 5c). These observations were confirmed by our study of synthetic $CaCO_3$:Eu. Hypersensitive $^5D_0$–$^7F_2$ (618 nm) emission dominates the Eu^{3+} luminescence spectrum, suggesting local Eu^{3+} ion coordination without inversion symmetry.

3.7. Scheelite $CaWO_4$

The Eu^{3+} luminescence spectrum of scheelite is similar to those recorded under steady-state conditions [2] and has a long decay time of 600 μs [10]. It is the only Eu^{3+} center detected in natural scheelite. Nevertheless, in synthetic $CaWO_4$, artificially activated by Eu in air and vacuum, three different Eu^{3+} are detected by time-resolved luminescence spectroscopy.

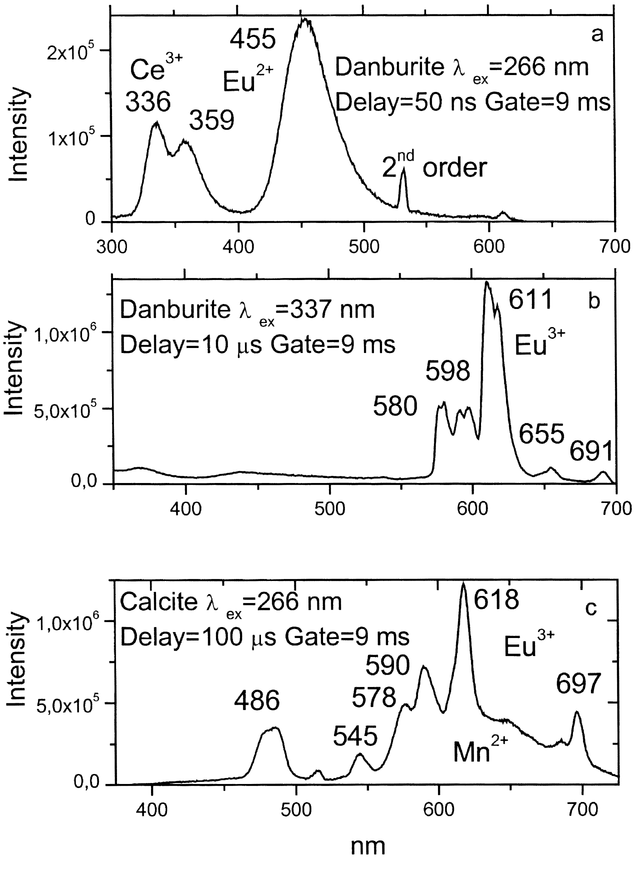

Fig. 5. Laser-induced time-resolved luminescence spectra under different excitations of danburite (a,b) and calcite (c).

4. Conclusions

Using laser-induced time-resolved spectroscopy, it is possible to detect very low concentrations (down to 0.1 ppm) of Eu in minerals and to determine its oxidation state and position in the lattice. The method is especially important in the cases of apatite and fluorite, which are the main luminescence indicators for the minerals formation. It is important to mention that in artificially activated apatite and fluorite, the luminescence of Eu^{3+} indicates that it is in a low symmetry position after activation in air. In contrast, the luminescence of Eu^{3+} indicates that it is in a high symmetry position after activation in reducing conditions in vacuum. One possible reason for this difference is having two ways of compensation for the excessive positive charge resulting from the Eu^{3+} for Ca^{2+} substitution. Under oxidizing conditions it may be an O^{2-} for F^- substitution, while under reducing conditions, the formation of Ca^{2+} vacancies may be preferable. In any case the detection of Eu^{2+} and Eu^{3+} in different lattice positions may greatly increase the scientific value of Eu impurity analysis because it may provide additional data on minerals origin and conditions of formation.

Acknowledgements

The Open University of Israel Research Fund supported this work.

References

[1] B. Gorobets, G. Walker, Origin of luminescence in minerals: a summary of fundamental studies and applications, in: A. Marfunin (Ed.), Advanced Mineralogy 2, Methods and Instrumentation, Springer, Berlin, Heidelberg, New York, 1995, pp. 138–146.

[2] A. Taraschan, in: Luminescence of Minerals, Naukova Dumka, Kiev, 1978, in Russian.

[3] G. Blasse, B. Grabmaier, in: Luminescent Materials, Springer, Berlin, Heidelberg, New York, 1994.

[4] R. Reisfeld, K. Jørgensen, in: Laser and Excited States of Rare Earths, Springer, Berlin, Heidelberg, New York, 1978.

[5] M. Kottaisamy, R. Jagannathan, P. Jeyagopal et al., J. Phys. D.: Apply. Phys. 27 (1994) 2210–2215.

[6] M. Gaft, R. Reisfeld, G. Panczer et al., J. Luminesc. 72–74 (1997) 572–574.

[7] I. Stepanov, P. Feofilov, DAN SSSR 108 (1956) 615–618, in Russian.

[8] M. Gaft, G. Panczer, R. Reisfeld et al., J. Luminesc. 87–89 (2000) 1032–1035.

[9] M. Gaft, in: Luminescence of Minerals Under Laser Excitation, Ministry of Geology, Moscow, 1989, in Russian.

[10] M. Gaft, G. Panczer, E. Uspensky, R. Reisfeld, Mineralogical Mag. 63–2 (1999) 199–210.